Characterization of structural dynamics of VO2 thin film on c-Al2O3 using in-air time-resolved x-ray diffraction

AUTHOR(S):

Hada, Masaki; Okimura, Kunio; Matsuo, Jiro

CITATION:

Hada, Masaki ...[et al]. Characterization of structural dynamics of VO2 thin film on c-Al2O3 using in-air time-resolved x-ray diffraction. Physical Review B 2010, 82(15): 153401.

ISSUE DATE:

2010-10

URL:

http://hdl.handle.net/2433/131852

PHYSICAL REVIEW B **82**, 153401 (2010)

Characterization of structural dynamics of VO_2 thin film on c-Al_2O_3 using in-air time-resolved x-ray diffraction

Masaki Hada*
Department of Nuclear Engineering, Kyoto University, Sakyo, Kyoto 606-8501, Japan

Kunio Okimura
Faculty of Engineering, Tokai University, Hiratsuka, Kanagawa 259-1292, Japan

Jiro Matsuo†
Quantum Science and Engineering Center, Kyoto University, Uji, Kyoto 611-0011, Japan
(Received 6 September 2010; published 5 October 2010)

The lattice motion and displacement of atoms in the unit cell in vanadium dioxide (VO_2) grown on c-Al_2O_3 were characterized by static and time-resolved x-ray diffraction (XRD) measurements. The monoclinic-tetragonal phase transition of the VO_2 unit cell and the twist motion of vanadium atoms in the unit cell were observed. The time-resolved XRD measurements were performed in air using a tabletop high-repetition femtosecond laser. The results obtained from the time-resolved XRD measurements suggested that the unit cell of the low-temperature monoclinic VO_2 transformed into the high-temperature tetragonal phase extremely rapidly (within 25 ps); however, the atoms in the unit cell fluctuated or vibrated about the center of the tetragonal coordinates, which abated within ~100 ps. Thus, the time-resolved XRD measurements of the Bragg angle, intensity, and width of the diffraction lines simultaneously revealed the phase transition of VO_2 and the atomic motion in the unit cell.

DOI: 10.1103/PhysRevB.82.153401 PACS number(s): 61.66.−f, 61.05.C−, 63.70.+h

Recently, time-resolved crystallography (x-ray diffraction[1–5] and electron diffraction[6–9]) has attracted considerable attention for its use in molecular-dynamical studies where it has been used to reveal chemical processes such as phase transitions and coherent phonon vibration in condensed matter. Vanadium dioxide (VO_2) is a representative material that undergoes a metal-insulator phase transition, which occurs at a temperature of ~340 K.[10] Several papers on optical,[11–13] terahertz,[14,15] and soft x-ray[16] spectroscopic pump-probe measurements of the phase transition in VO_2 have been reported and a few reports on time-resolved crystallography reveled the intriguing nature of the structural dynamics of the phase transition in VO_2. A phase transition was observed in a bulk sample by the changes in intensity of x-ray diffraction lines from around the (011) plane[17] and in a thin-film sample by the changes in intensity of several electron-diffraction spots.[18] In this study, we performed time-resolved x-ray diffraction (XRD) measurements of the photo-induced phase transition in an epitixial VO_2 thin film on c-Al_2O_3. The analysis based on complicated XRD data enabled the separation of the motion in the VO_2 film, the lattice unit cells and the atoms in the unit cell, enabling us to directly observe not only the phase transition of the unit cell but also the displacement of atoms in the unit cell at a picosecond time scale. A series of direct structural observations reveals the transition states of the phase-transition materials and it is expected that in the future the mechanism of the photo-induced nonequilibrium process will be clarified.

A highly (010) oriented VO_2 film (280 nm thickness) was epitaxially grown on a c-Al_2O_3 (0001) substrate at a temperature of 673 K.[19,20] Static out-of-plane and in-plane XRD measurements with Cu $K\alpha$ x-ray radiation (λ=0.154 nm) were performed at temperatures of 293 K (low-temperature phase) and 343 K (high-temperature phase) using an x-ray diffractometer. The monoclinic and tetragonal VO_2 structures reside in the space groups of $P2_1/C$ (No. 14) (Ref. 21) and $P4_2/mnm$ (No. 136),[22] respectively. Figure 1 shows the lattice parameters and atomic coordinates determined from the static XRD lines of (020), (040), (200), (022), and (40–2). The lattice parameters were calculated from the Bragg equation and the Bragg angle obtained from results of static XRD measurements. The atomic coordinates in the unit cell were calculated on the basis of Ref. 23 by the computer simulation using CRYSTALMAKER 8.2 with the relative integral intensity of each diffraction line.[24,25] The simulation software calculates the Bragg angle and the relative intensity of the diffraction lines from the Bragg equation and Eqs. (1)–(3). These lattice parameters were slightly destorted (0.1–0.5 % for each axis) from those reported for VO_2 powder[21–23] because of the effect of tension from the substrate.

The static XRD measurement also revealed structure changes in VO_2 before and after the transition. The intensity of the diffraction line (I) can be defined as

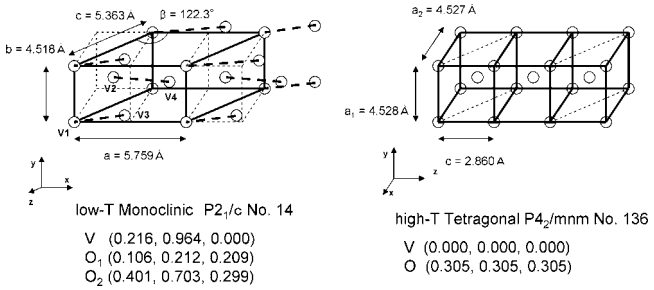

FIG. 1. The lattice parameters and positions of vanadium atoms in the unit cell of the epixially grown VO_2 thin film.

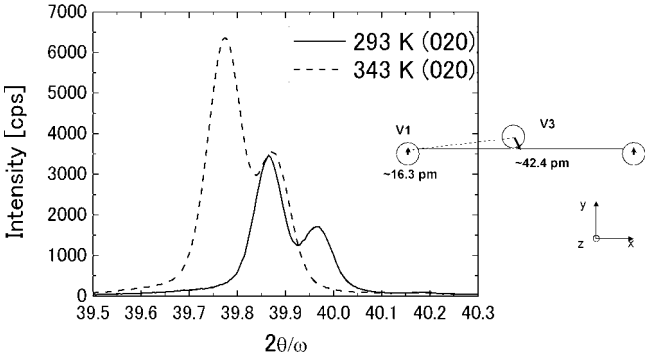

FIG. 2. The spectra of the static out-of-plane XRD lines from the (020) plane of the VO_2 sample at temperatures of 293 K (monoclinic phase) and 343 K (tetragonal phase). The change in the unit cell induced the change in the Bragg angle and the changes in the atomic position increased the intensity of diffraction lines.

$$I = G(\vec{K})^2 F(\vec{K})^2, \tag{1}$$

$$G(\vec{K}) = \sum_{u,v,w} \exp[2\pi i \vec{K} \cdot (u\vec{a} + v\vec{b} + w\vec{c})], \tag{2}$$

$$F(\vec{K}) = \sum_{j=1} f_j(\vec{K}) T_j(\vec{K} \exp[2\pi i \vec{K} \cdot r_j], \tag{3}$$

where $\vec{K}$, $G(\vec{K})$, $F(\vec{K})$, $f_j(\vec{K})$, and $T_j(\vec{K})$ are the wave vector, Laue function, crystal-structure factor, atomic-scattering factor, and temperature factor, respectively. The position of each atom in the unit cell is represented as $\vec{r_j}$. The Bragg angle of the diffraction line depends on the Laue function [Eq. (2)]; more specifically, it depends on the size of the unit cell. In contrast, the intensity of the diffraction line strongly depends on the crystal structure factor [Eq. (3)]. The differences in the atomic scattering factor and temperature factor before and after the transition are negligible; therefore, the intensity of the diffraction line mainly depends on the positions of the atoms in the unit cell. Figure 2 shows the Cu $K\alpha$ XRD lines at low temperatures (2θ=39.86°) and high temperatures (2θ=39.77°) obtained from the VO_2 (020) plane. The changes in Bragg angle and intensity were relatively large in the diffraction lines from the (020) plane among the observed diffraction lines. In Fig. 2, the diffraction lines shifted 0.09° toward a lower angle in the high-temperature phase as a result of the upswelling of the unit cells which was estimated to be 1.0 pm in the y direction. The integral intensity of the diffraction lines increased ~2.2-fold in the high-temperature phase, mostly as a result of the improved symmetry of the atomic positions in the unit cell. The change in the atomic positions can be estimated from the atomic coordinates shown in Fig. 1. There are four vanadium atoms in a unit cell, V1, located near the corner of the unit cell, and V2, near the center of the (011) plane, moved ~16.3 pm in opposite directions parallel to the y axis, and V3 and V4 changed the positions by moving a distance of ~42.4 pm. These results agreed with the relative magnitudes in reference,[23] in which V1 and V2 moved ~10 pm and V3 and V4 moved ~22 pm. The atomic pairs V1–V3 and V2–V4 in the monoclinic phase made twist movements.

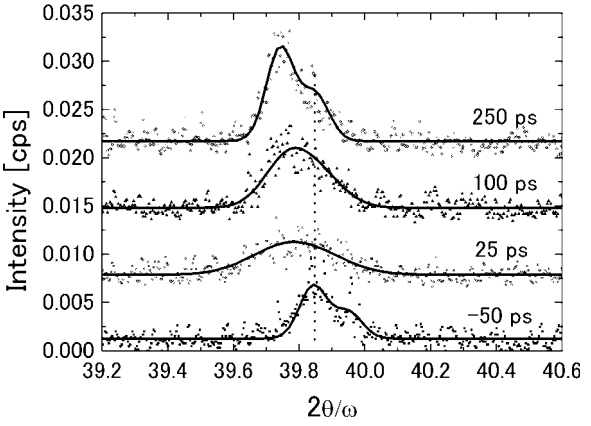

FIG. 3. The typical spectra of the time-resolved XRD lines from the (020) plane of the VO_2 sample; the vertical line shows the Bragg angle of VO_2 for a negative time delay. The solid lines are fitting curves of the double Gaussian, where the $K\alpha_1$ and $K\alpha_2$ XRD lines are represented.

Time-resolved XRD measurements were performed in air using a laser-plasma-induced x-ray source of Cu $K\alpha_1$ and $K\alpha_2$ radiation at 1 kHz, generated by focusing a millijoule femtosecond laser onto a rotating copper target in helium ambient.[26,27] The measurements were assembled with a compact designed XRD system with a tabletop femtosecond laser. The probing x-ray radiation emitted over a range of 2π steradians was collimated using slits with 0.3 mm width and 1 mm height, and was focused on the VO_2 sample at an incident angle of 19.91° to detect diffraction lines from the (020) plane. The pulse width of the pulsed x-ray was estimated to be about 200 fs (Ref. 28) and the time resolution was about 1 ps, determined by considering the geometry of x-ray divergence angle. The diffracted x-ray was detected using a charge coupled device camera. The VO_2 sample was loaded on a thermal heater, the temperature of which was controlled at 316 K. The sample was photo excited using an 800-nm-wavelength femtosecond optical pulse. The area excited by the optical pulse had a 1.7 mm diameter and was larger than the x-ray-probed area. The intensity of the pumping pulse was 8.7 mJ/cm^2, higher than the phase transition threshold (6–7 mJ/cm^2) (Refs. 17 and 18) and much lower than the single-shot damage threshold (63 mJ/cm^2).[17]

The typical XRD spectra at time delays of −50, 25, 100, and 250 ps are shown in Fig. 3. As shown in the figure, the Bragg angle of the diffraction lines was higher for the negative delay time and it shifted toward a markedly lower angle at 250 ps. The integral intensity of the diffraction lines was doubled by through the transition. These changes corresponded well to those observed in the static XRD measurements. The time-resolved XRD measurements enabled us to obtain information on the disequilibrium state of VO_2, i.e., the diffraction lines at 25 ps. Figures 4(a)–4(c), which were derived from Fig. 3, show the changes in the Bragg angle, integral intensity and full width at half maximum (FWHM) of the diffraction lines as a function of delay time. As shown in Figs. 4(a) and 4(b), the Bragg angle of the diffraction lines shifted toward a lower angle within 25 ps; on the other hand,

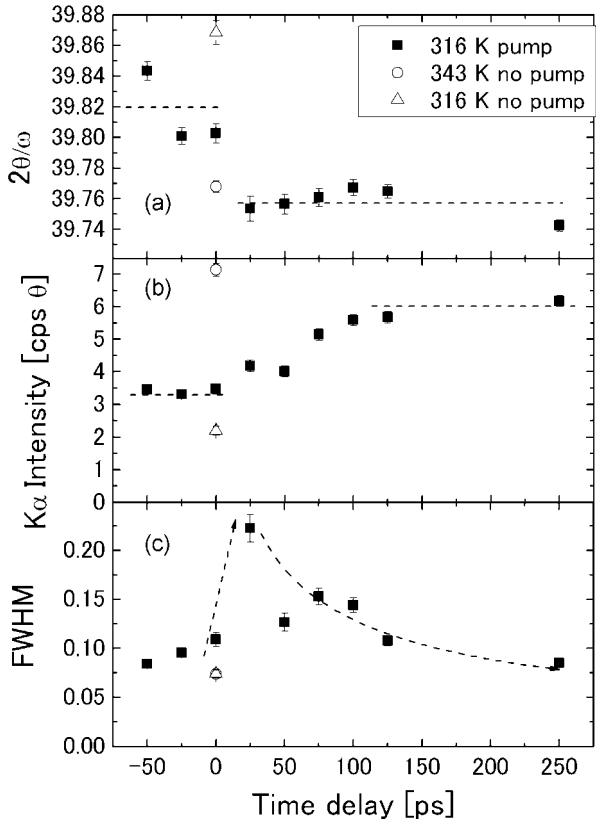

FIG. 4. (a) The changes in the Bragg angle, (b) the integral intensity, and (c) the FWHM of the (020) XRD lines. The dotted lines are guides to the eye.

the integrated intensity gradually increased up to ~100 ps. The FWHM of the diffraction lines increased by a factor of 2–3 in the first 25 ps then gradually decreased during the following ~100 ps [Fig. 4(c)]. The change in the Bragg angle of the diffraction lines suggests that the VO_2 monoclinic unit cell transformed into a tetragonal unit cell extremely rapidly (within 25 ps). To analyze the changes in the intensity and FWHM of the diffraction lines, the fluctuation in film depth should be considered because the penetration depth of the optical pulse at a wavelength of 800 nm was shallower than the film thickness. The complex refractive index of VO_2 in the insulator phase was $2.9-0.385i$ (the wavelength: 800 nm);[29] therefore, the $1/e$ penetration depth of the optical pulse was calculated to be 163 nm at an incident angle of 30°. Regarding the fluctuation in film depth, we made the simple assumption that the upper half of the film was excited and underwent a transition to the tetragonal phase, whereas the lower half remained in the monoclinic phase in the transition state. The photoexcited layer propagated to the deeper part of the film at the acoustic velocity of ~100 nm per ~100 ps, which was consistent with the previously reported results.[17,18,30] With this assumption, the diffraction line in the transition state should be a combination of diffraction lines from the monoclinic and tetragonal phases in the ultrafast time scale. The increasing in the FWHM of diffraction lines may have been induced with the propagation of photoexcited layer. However, the peak intensity of the diffraction lines from the tetragonal phase in the upper half of the film and the monoclinic phase in the lower half should be higher than those from the monoclinic phase. Therefore, the reduction in the peak intensity of the diffraction line shown in Fig. 3 (at 25 ps) cannot be explained only by this photoexcited layer propagation. The change in the Bragg angle occurred at an ultrafast time scale (<10 ps) in the XRD measurements performed by Cavalleri *et al.*[17] and the corresponding changes in Bragg angle corresponded well to our results. However, it was difficult to discuss the atomic motion which can be estimated from the change in intensity because the film in reference[17] was much thicker (~2 μm) than the $1/e$ penetration depth.

The increase in the FWHM of the diffraction lines has been induced by the fluctuation of the unit cells. According to Eq. (2), the superposition of unit cells of different size can also produce diffraction lines with an increased FWHM. This interunit-cell fluctuation was driven by the displacement of atoms in the unit cell by long distance (~10 pm) in short time (less than 25 ps). If the fluctuation in the unit cell was driven by the displaced atoms, which caused the increase in the FWHM of the diffraction lines, the intensity of the diffraction lines should be decreased simultaneously because the atomic fluctuation reduces the intensity of the diffraction lines according to Eq. (3). As shown in Fig. 3 shows, the peak intensity of the diffraction lines at 25 ps was reduced by about half. The fluctuations of the unit cell and atoms in the unit cell are thought to gradually abate by thermal coupling in ~100 ps, which should lead to a decrease in the FWHM of the diffraction lines and an increase in their peak intensity. The fluctuation or vibration might be the similar nature observed in the spectroscopic methods.[13–16] The transition state would be a very complex state involving "phase transition," "photoexcited layer propagation," and "fluctuation or vibration." Cavalleri *et al.*[17] and Baum *et al.*[18] showed that the phase transition in VO_2 mainly occurs within ~12 ps and by less than 500 fs, respectively, which are consistent with this phase transition time scale of less than 25 ps. Here, it is worth mentioning that in this study the Bragg angle, intensity, and FWHM of the diffraction lines from the (020) plane of the VO_2 thin film were measured by stimulatory time-resolved XRD, which revealed the fluctuation or vibration of the VO_2 lattice and the atoms in the unit cell. The time-resolved electron-diffraction measurements revealed a change in the intensity of several diffraction spots with a very high time resolution; however, the displacement of the unit cell of VO_2 was ~1.0 pm, therefore the change in the diffraction angle can be calculated to be ~0.03°. The change in Bragg angle of ~0.03° corresponded to ~180 μm on the multichannel plate at the camera length of 300 mm, which is difficult to resolve with electron diffraction measurements because the electron beam size was ~200 μm.[31] However, the change in Bragg angle of about ~0.1° can be easily resolved with x-ray diffraction measurements. In conclusion, the transition state of a photoexcited VO_2 thin film, which appeared only in the extremely fast time scale, was investigated by time-resolved XRD using a tabletop system. The fluctuation or vibration has been observed only in the spectroscopic methods; however, it was observed using more direct XRD measurement with the changes in the intensity and FWHM of the diffraction lines. The photoexcited monoclinic

VO_2 was transmitted into a tetragonal structure rapidly; however, the atoms in the unit cell and the unit cell itself fluctuated or vibrated around the center of the tetragonal coordinates. The atomic fluctuation was coupled with an isotropic thermal phonon and abated in ~100 ps. The photoexcited layer propagation would be a competitive process in this time scale. The results also suggest that the tabletop time-resolved XRD system is a promising tool for laboratory-based molecular-dynamics studies on materials, chemical, and biological systems.

This work was partially supported by Core Research for Evolutional Science and Technology (CREST) of the Japan Science and Technology Agency (JST). The author would like to thank R. Manory of editassociates.com for help with preparing this material for publication.

*hadamasaki@nucleng.kyoto-u.ac.jp
†matsuo@nucleng.kyoto-u.ac.jp

[1] C. Rose-Petruck *et al.*, Nature (London) **398**, 310 (1999).
[2] K. Sokolowski-Tinten *et al.*, Nature (London) **422**, 287 (2003).
[3] A. M. Lindenberg *et al.*, Science **308**, 392 (2005).
[4] D. M. Fritz *et al.*, Science **315**, 633 (2007).
[5] K. Sokolowski-Tinten and D. von der Linde, J. Phys.: Condens. Matter **16**, R1517 (2004).
[6] H. E. Elsayed-Ali and G. A. Mourou, Appl. Phys. Lett. **52**, 103 (1988).
[7] B. J. Siwick, J. R. Dwyer, R. E. Jordan, and R. J. D. Miller, Science **302**, 1382 (2003).
[8] H. Park, X. Wang, S. Nie, R. Clinite, and J. Cao, Phys. Rev. B **72**, 100301 (2005).
[9] F. Carbone, P. Baum, P. Rudolf, and A. H. Zewail, Phys. Rev. Lett. **100**, 035501 (2008).
[10] F. Morin, Phys. Rev. Lett. **3**, 34 (1959).
[11] M. F. Becker, A. B. Buckman, R. M. Walser, T. Lepine, P. Georges, and A. Brun, Appl. Phys. Lett. **65**, 1507 (1994).
[12] S. Lysenko, A. J. Rua, V. Vikhnin, J. Jimenez, F. Fernandez, and H. Lu, Appl. Surf. Sci. **252**, 5512 (2006).
[13] H.-T. Kim, Y. W. Lee, B.-J. Kim, B.-G. Chae, S. J. Yun, K.-Y. Kang, K.-J. Han, K.-J. Yee, and Y.-S. Lim, Phys. Rev. Lett. **97**, 266401 (2006).
[14] C. Kübler, H. Ehrke, R. Huber, R. Lopez, A. Halabica, R. F. Haglund, Jr., and A. Leitenstorfer, Phys. Rev. Lett. **99**, 116401 (2007).
[15] M. Nakajima, N. Takubo, Z. Hiroi, Y. Ueda, and T. Suemoto, J. Lumin. **129**, 1802 (2009).
[16] A. Cavalleri, M. Rini, H. H. W. Chong, S. Fourmaux, T. E. Glover, P. A. Heimann, J. C. Kieffer, and R. W. Schoenlein, Phys. Rev. Lett. **95**, 067405 (2005).
[17] A. Cavalleri, Cs. Toth, C. W. Siders, J. A. Squier, F. Raksi, P. Forget, and J. C. Kieffer, Phys. Rev. Lett. **87**, 237401 (2001).
[18] P. Baum, D.-S. Yang, and A. H. Zewail, Science **318**, 788 (2007).
[19] K. Okimura and J. Sakai, Jpn. J. Appl. Phys. **48**, 045504 (2009).
[20] K. Okimura, N. Ezreena, Y. Sasagawa, and J. Sakai, Jpn. J. Appl. Phys. **48**, 065003 (2009).
[21] G. Andersson, Acta Chem. Scand. **10**, 623 (1956).
[22] S. Westman, Acta Chem. Scand. **15**, 217 (1961).
[23] J. M. Longo and P. Kierkegaard, Acta Chem. Scand. **24**, 420 (1970).
[24] CrystalMaker Software Limited, CRYSTALMAKER 8.2, http://www.crystalmaker.com/
[25] M. Israelsson and L. Kihlborg, Mater. Res. Bull. **5**, 19 (1970).
[26] M. Hada and J. Matsuo, Trans. Mater. Res. Soc. Jpn. **34**, 621 (2009).
[27] M. Hada and J. Matsuo, Appl. Phys. B: Lasers Opt. **99**, 173 (2010).
[28] Ch. Reich, P. Gibbon, I. Uschmann, and E. Förster, Phys. Rev. Lett. **84**, 4846 (2000).
[29] M. Tazawa, P. Jin, and S. Tanemura, Appl. Opt. **37**, 1858 (1998).
[30] M. S. Grinolds, V. A. Lobastov, J. Weissenrieder, and A. H. Zewail, Proc. Natl. Acad. Sci. U.S.A. **103**, 18427 (2006).
[31] N. Gedik, D.-S. Yang, G. Longvenov, I. Bozovic, and A. H. Zewail, Science **316**, 425 (2007).